28 July 1995

ELSEVIER

Chemical Physics Letters 241 (1995) 301–310

CHEMICAL PHYSICS LETTERS

$^{13}C/^{12}C$ ratio measurements of aromatic molecules using photoionization with TOF mass spectrometry

C.R. Maechling, S.J. Clemett, R.N. Zare

Department of Chemistry, Stanford University, Stanford, CA 94305-5080, USA

Received 2 March 1995; in final form 8 May 1995

Abstract

We demonstrate a method for measuring the carbon isotope ratios of aromatic molecules without the need for chemical preparation. The technique employs a time-of-flight (TOF) mass spectrometer equipped with a dual microchannel plate detector assembly. We present the measurement of carbon isotope ratios for *m*-xylene-d_{10} ($C_6D_4(CD_3)_2$), toluene ($C_6H_5CH_3$), and toluene-d_8 ($C_6D_5CD_3$). Gas-phase samples are photoionized with the 266 nm output of a Nd:YAG laser, and the abundance of ^{12}C and ^{13}C in the molecules is derived from the TOF spectra. Complications caused by and corrections for detector nonlinearity and parent ion fragmentation are discussed.

1. Introduction

Stable isotope ratio analysis is an important tool for geology, meteoritics, medicine, biology, ecology, and environmental science [1–4]. The stable isotopes of carbon are ^{12}C and ^{13}C, and their isotope ratio R is defined by

$$R = \left(\frac{^{13}C}{^{12}C} \right). \quad (1)$$

The variation of R is small, ranging from 0.0107 to 0.0113, for carbon-containing samples found on Earth. The fractional deviation of R for a sample from R for a standard in parts per thousand is called the *delta scale* and is reported in units of per mil (‰):

$$\delta^{13}C = \frac{(R - R_{\text{standard}})}{R_{\text{standard}}} 1000 \quad (2)$$

where R_{standard} for the terrestrial standard, Pee Dee Belemnite, is 0.0112372 ± 0.0000090 [5].

Conventional stable carbon isotope analysis involves combusting a carbon-containing sample and analyzing the isotopic composition of the resulting CO_2. Typically, high-precision mass spectrometers [6] are used to record the isotopomers (molecules composed of nuclei with identical atom numbers and differing mass numbers) of CO_2; however, laser methods based on the isotopic shift in spectral lines have been used as well [7]. For samples containing complex mixtures of carbon-containing compounds, each component may have a different carbon isotope ratio and must be separated so as not to obscure the isotopic evidence. One method of high-precision compound-specific isotope analysis involves coupling a gas chromatograph to a combustion furnace followed by a high-precision isotope ratio mass spectrometer (IRMS) [8]. Gas chromatography–combustion–IRMS can analyze carbon isotope ratios to 0.5 per mil for any component of the mixture that has been chromatographically resolved from the other components; however, the effluent from the gas

SSDI 0009-2614(95)00590-0

chromatograph must contain several picomoles of the component to achieve this level of precision [9].

Although carbon isotope ratios for carbon-containing samples from terrestrial environments lie in a narrow range (between -50 and $+5$ per mil), microscopic specimens from distant stellar bodies have recently been found to contain 'exotic' abundances of the carbon isotopes. For example, interstellar graphite grains showing dramatic bulk carbon enrichments (as large as $+43000‰$) and depletions (as small as $-950‰$) of $\delta^{13}C$ have been discovered in the Murchison meteorite [10]. To determine whether the organic compounds associated with these grains carry a similar isotopic signature requires only modest precision but extremely high sensitivity and molecular selectivity.

We present here a new method for compound-specific carbon isotope ratio analysis using photoionization with time-of-flight (TOF) mass spectrometry. The photoionization step enables specific classes of molecules to be selected and TOF mass spectrometry separates the selected class of molecules by their mass. For each laser shot, ions of all the isotopomers are separated and simultaneously recorded. Although TOF mass spectrometry is a very sensitive technique, it is not known for extremely accurate isotope analysis. We find, however, that TOF mass spectrometry can determine carbon isotope ratios to a precision of better than 30 per mil.

Using this technique in combination with laser desorption [11,12], we can attempt to perform carbon isotope measurements on samples of limited size including interstellar graphite grains which may contain small concentrations of aromatic molecules with exotic abundances of the carbon isotopes. For the gas-phase experiments presented here, we present carbon isotope ratio analyses using both analog and ion counting modes of our microchannel plate (MCP) detector assembly. For two-step experiments, we will rely on determining carbon isotope ratios from the analog signal collection mode. Owing to the pulsed nature of the two-step experiments, the few molecules that may exist on microscopic samples are desorbed in 'bunches' and must be collected in an analog mode.

In this Letter, we discuss how to obtain carbon isotope ratios from the data recorded with our instrument and present results for toluene (methylbenzene, $C_6H_5CH_3$), toluene-d_8 ($C_6D_5CD_3$), and *m*-xylene-d_{10} (dimethylbenzene, $C_6D_4(CD_3)_2$). In addition to producing parent ions, the photoionization step can generate fragment ions. The fragment ions of toluene-d_8 and *m*-xylene-d_{10} do not share a common mass with peaks used for carbon isotope ratio analysis, whereas fragment ions of toluene overlap with peaks used in the analysis. Because of their interference-free isotopomer mass peaks, toluene-d_8 and *m*-xylene-d_{10} were investigated to demonstrate the efficacy of our method, whereas toluene was studied to identify a method for deconvoluting the contributions from fragment ions in our carbon isotope ratio analysis.

2. Experimental

The TOF instrument used for this study is displayed in Fig. 1. Sample gases were backfilled into the chamber ($< 1 \times 10^{-8}$ Torr) and ionized by resonance-enhanced multiphoton ionization (REMPI) using the fourth harmonic of a Nd:YAG laser (266 nm). The pulse energy of the laser, and thus the number of ions produced per laser shot, was controlled by changing the laser *Q*-switch delay. The ions were produced in a modified Wiley–McLaren extraction region [13], reflected with a two-stage reflectron, and detected by a chevron configuration MCP assembly. Ions were produced in the source at a repetition rate of 10 Hz. The output of the detector was amplified with a direct-coupled preamplifier ($\times 10$), and the signal was recorded in either analog or ion counting modes.

2.1. Detection methods

The method we choose to record signal from the preamplifier depends on the flux of ions reaching the MCP assembly. In the case that less than one ion of a given mass is observed for every laser shot, we count ions using a multichannel scaler. For greater ion currents, we 'shape' the pulses using a 20 ns integration filter and measure the time-dependent voltage on a 350 MHz digital oscilloscope.

Ion counting was performed using a multichannel scaler which counts the number of times an ion, larger than the discriminator level, reaches the detec-

tor during a specific 5 ns bin. Because the probability of observing an ion that impacts upon the detector is essentially unity, the accuracy of the ion distribution measurements is limited only by counting statistics, and therefore, it is improved by counting more ions. This improvement is accomplished by increasing the number of laser shots, and hence the data accumulation time. To achieve a precision of 16 per mil with our data acquisition rate of 10 Hz, approximately 10 h of continuous operation was needed.

When several ions reach the detector simultaneously, the total current produced by the detector assembly is roughly proportional to the number of ions impinging upon the detector. To determine isotope ratios the exact relationship between the current and the ion flux must be understood. For analog detection, a digital oscilloscope was used to sample the shaped detector output every 2.5 ns and record a complete TOF trace for each laser shot. Spectra were averaged in a built-in, 'summed averaging' program provided with the oscilloscope. Summed averaging consists of repeated addition, with equal weight, of successive source waveform records. The accuracy of an isotope measurement is related to how accurately the output of the detector can be digitized. The 8-bit resolution of the flash converters in the oscilloscope causes the voltage (signal current measured across a resistor) to be measured to only 1 part in 256; however, signal averaging improves the signal-to-noise ratio and the 'effective resolution' of our analog measurements. Our oscilloscope is capable of

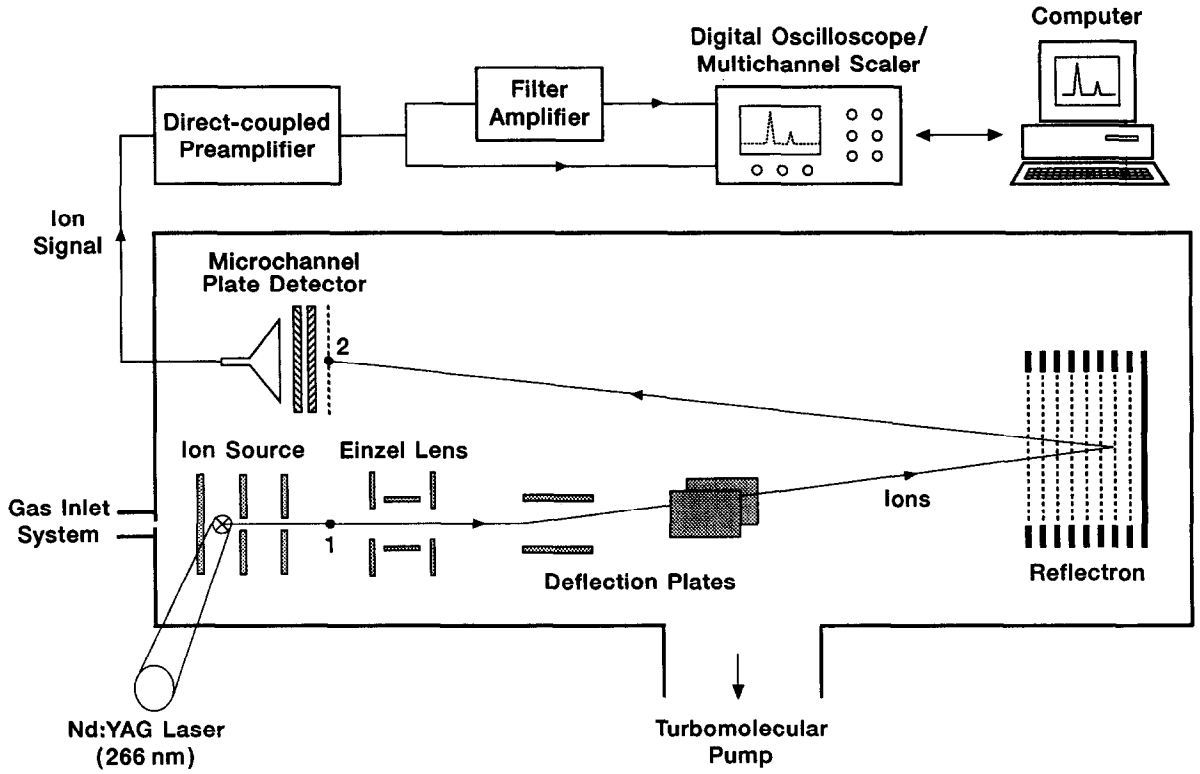

Fig. 1. Schematic of photoionization TOF mass spectrometer. The chamber is pumped with a turbomolecular pump to a base pressure of (1×10^{-8} Torr). Sample is introduced through a leak valve on the gas inlet system and photoionized in the extraction region of a modified Wiley–McLaren ion source. Ions are brought to a primary focus at 1, steered to a reflectron mirror, and reflected back to a secondary focus 2. A dual microchannel plate detector in a chevron configuration is located at the secondary focus. For small ion currents, ion signal is amplified with a direct-coupled preamplifier ($\times 10$) and recorded on a multichannel scaler. For large ion currents, ion signal is amplified with a direct-coupled preamplifier ($\times 10$) and a filter amplifier ($\times 2$, 20 ns integration) and recorded on a digital oscilloscope. Data files are transferred to a computer from both detector units.

recording averaged traces with 16-bit resolution, but for the number of traces and size of the signals we observed, we operated with 12-bit effective resolution. We have performed simulations of the quantization error associated with 12-bit resolution and found carbon isotope ratios can be determined to within 5 per mil.

3. Distribution of isotopomers

Isotopomers in organic compounds arise from isotopic abundance, which is predominantly ^{13}C substituting for ^{12}C at roughly 1.1% for terrestrial abundance. For toluene-d_8 and *m*-xylene-d_{10}, the isotopomer distribution is exclusively the result of the carbon isotope abundances. For toluene, the isotopomer distribution results from the carbon and hydrogen isotope abundances. Because the terrestrial abundance of D in hydrogen is 0.002%, three orders of magnitude smaller than the abundance of ^{13}C in carbon, we can exclude it from discussion [14].

The largest portion of toluene-d_8 molecules is $^{12}C_7D_8$, with a smaller amount of $^{13}C_1{}^{12}C_6D_8$, and an even smaller amount of $^{13}C_2{}^{12}C_5D_8$. The abundances of the various isotopomers are predicted by binomial statistics, in which the probability of finding ν ^{13}C atoms in a molecule containing n carbon atoms is given by

$$P(\nu\ ^{13}\mathrm{C}\ \text{in}\ n\ \text{sites}) = \binom{n}{\nu} a^{\nu} b^{n-\nu}, \tag{3}$$

where a is the fraction of carbon that is ^{12}C, b is the fraction of carbon that is ^{13}C, n is the number of carbons in the molecule, ν is the number of carbon sites that contain ^{13}C, and

$$\binom{n}{\nu} = \frac{n!}{\nu!(n-\nu)!}. \tag{4}$$

The sum of the probabilities for the $n+1$ isotopomer terms can also be described by the binomial expansion [15],

$$\begin{aligned}\sum_{\nu=0}^{n} \binom{n}{\nu} a^{\nu} b^{n-\nu} &= (a+b)^n \\ &= a^n + n a^{n-1} b + \frac{n(n-1)a^{n-2}b^2}{2!} \\ &\quad + \frac{n(n-1)(n-2)a^{n-3}b^3}{3!} + \ldots . \end{aligned} \tag{5}$$

Assuming that the toluene-d_8 was created from carbon of terrestrial abundance [12] ($a = 0.9889$, $b = 0.0111$, $n = 7$), the statistical distribution of isotopomers would appear as found in Table 1. The isotopomer labels used in Table 1 are general for all isotopomer distributions. The isotopomer that contains all ^{12}C is labeled M and is described by the first term of the expansion found in Eq. (5), the isotopomer that contains one ^{13}C atom is labeled (M + 1) and is described by the second term in the expansion, and so forth. The ratio of abundances for any two isotopomers can therefore be used to determine the isotope ratio of the molecule,

$$\frac{\text{abundance(M+1)}}{\text{abundance(M)}} = n\frac{b}{a}, \tag{6}$$

$$\frac{\text{abundance(M+2)}}{\text{abundance(M)}} = \tfrac{1}{2}n(n-1)\left(\frac{b}{a}\right)^2, \tag{7}$$

etc. The abundances are determined from the experiment, the number of carbons n is defined by the molecule, and the ratio of b to a defines R. We can therefore find the carbon isotope ratio R from Eq. (6),

$$R = \frac{b}{a} = \frac{\text{abundance(M+1)}}{n[\text{abundance(M)}]}. \tag{8}$$

The ratio R is then used in Eq. (2) to determine the carbon isotope ratio in the delta scale.

Table 1
Isotopomers of the molecule toluene-d_8

Mass (amu)	Isotopomer composition	Isotopomer label	Relative abundance
100	$^{12}C_7D_8^{13}$	M	100
101	$C_1^{12}C_6D_8^{13}$	(M+1)	7.7
102	$C_2^{12}C_5D_8^{13}$	(M+2)	0.25
103	$C_3^{12}C_4D_8^{13}$	(M+3)	5×10^{-3}
104	$C_4^{12}C_3D_8^{13}$	(M+4)	5×10^{-5}
105	$C_5^{12}C_2D_8^{13}$	(M+5)	3×10^{-7}
106	$C_6^{12}C_1D_8$	(M+6)	1×10^{-9}
107	$^{13}C_7D_8$	(M+7)	2×10^{-11}

3.1. Discrimination effects

The carbon isotope ratio is measured with our instrument by photoionizing the neutral molecules, separating the ions by mass, and detecting the various ions. Photoionization generates predominately parent ions, although fragment ions are generated as well. From power dependence studies, we determined that the ionization of toluene-d_8 and toluene are two-photon processes, whereas the easiest fragmentation schemes (deuterium and hydrogen loss, respectively) are three-photon processes. Fragment ions will always be present, although the extent to which they are present can be controlled with the laser power. A schematic of the fragmentation process for toluene and toluene-d_8 are shown in Fig. 2a and 2b.

To derive the neutral populations of toluene-d_8 from the mass spectra, the following assumptions are made:

–The probability of ionization for M and (M + 1) is the same.

–The probability of deuterium loss from M and (M + 1) is the same.

–The detector response to M^+ and $(M + 1)^+$ is the same.

–There are no fragmentation interferences at masses 100 and 101 amu because fragments having lost one deuterium atom which result simultaneously with photoionization appear at masses 98 and 99 amu.

In theory, the distribution of observed ions (M^+ and $(M + 1)^+$) should be identical to the distributions of neutrals (M and (M + 1)). In experiment, however, discrimination effects can occur.

Because we are trying to establish the distribution of neutral molecules from our recorded ion signal, we must determine all possible sources of bias. No discrimination effects are expected from introducing the vapor into the instrument, photoionizing the neutrals, or mass separating the ions, but attention must be given to the series of events that occur at the microchannel plate assembly. When a packet of ions of a given mass arrives at the microchannel plate detector, it creates a current that, when integrated, is roughly proportional to the number of ions in the packet. If we wish to obtain the accuracy needed to measure significant isotope ratios, however, great

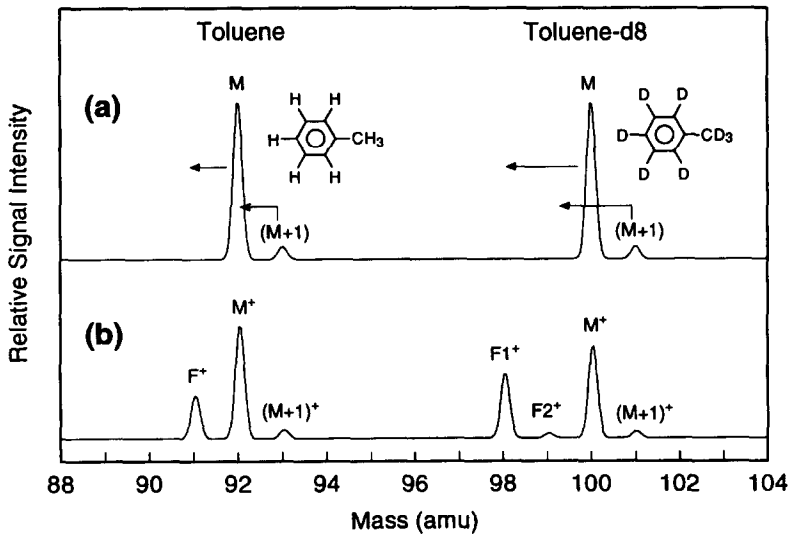

Fig. 2. Schematic of toluene and toluene-d_8 fragmentation effects. The neutral distribution would be accurately portrayed in the mass spectrum (a) except that the pulsed laser beam fragments the isotopomers. Fragmentation does not cause interferences in the toluene-d_8 mass spectrum (b), and the ratio of $(M + 1)^+$ to M^+ is equivalent to the ratio of (M + 1) to M. However, fragmentation does cause interferences in the toluene mass spectrum (b) because M^+ contains fragments from (M + 1). Fragment peaks not coinciding with the M^+ or $(M + 1)^+$ peaks are labelled F^+, $F1^+$, and $F2^+$.

care must be taken when we relate the integrated current detected to the number of ions present. The two most serious causes of discrimination are the nonlinear amplification of the microchannel plates and the method of detection. If the flux of ions is kept small enough so that ion counting can be performed, almost no discrimination can occur. Because the frequency of ions reaching the detector is low, the gain for every detection event is equivalent. Although ion counting solves the problem of detector nonlinearity, the reduced flux of ions causes the experiment to be impractical for the measurement of microscopic samples that contain few molecules of interest. We must, therefore, consider analog collection and the complications of nonlinearity.

The principal form of nonlinearity is wall charge gain saturation, or pulse pileup. When an incident ion impinges upon a channel of an MCP, secondary electrons are generated and accelerated along the channel causing an electron cascade and liberating more secondary electrons. This process continues until a charge cloud of typically 10^3 electrons exits the backside of the plate. Pulse pileup occurs when the charge extracted from the wall by the front-end of a pulse is not completely replenished in time for the tail-end of that pulse because the recharge time constant for the channel is longer than the temporal spread of the pulse. Therefore, the tail-end of the pulse is slightly less amplified than the front-end. As the ion current arriving at the MCP increases, the pileup worsens. In addition, subsequent pulses arriving at the detector may experience reduced amplification, depending on their arrival times. We expect that the detector response function should be unity for low ion currents and approach zero for high ion currents. The functional form of the response of an MCP plate, $G(s)$, where s is proportional to the total charge of the impinging pulse, has been reported from both experiments and theory [16] to be given by:

$$G(s) = \frac{\ln(1+s)}{s}. \tag{9}$$

Because the abundance of the toluene-d_8 isotopomer (M + 1) is roughly 7.7% that of the isotopomer M, the response of the detector as a function of signal must be characterized.

4. Results and discussion

4.1. Ion counting

The carbon isotope ratio of toluene-d_8 was calculated from the 42775 M^+ ions and 3275 $(M+1)^+$

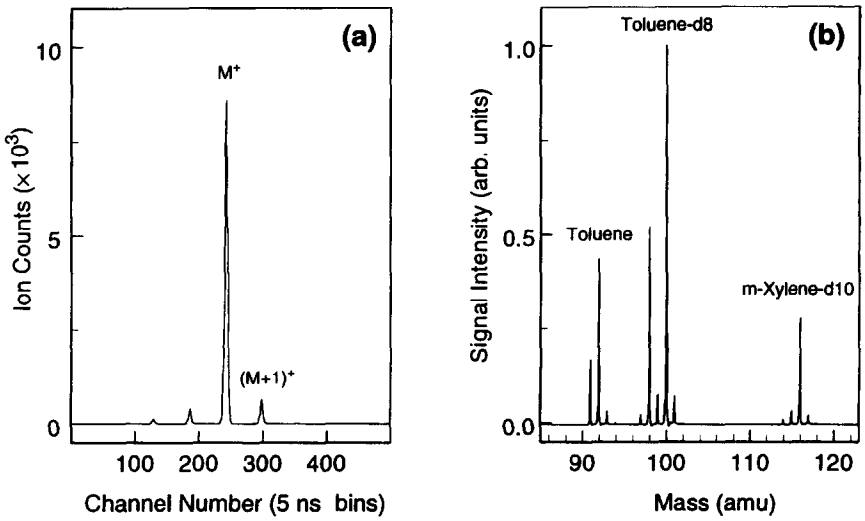

Fig. 3. Representative time-of-flight spectra used to determine the carbon isotope ratios for aromatic molecules. Ion counting with 5 ns channel widths was used to acquire (a) for toluene-d_8. Analog detection was used to acquire (b) for a mixture of toluene, toluene-d_8, and m-xylene-d_{10}. Fragments from the parents ions are observed to the left of each parent.

ions produced by 3.13×10^5 laser shots. The output from the multichannel scaler is displayed in Fig. 3a. To determine the isotope ratio R we used Eq. (8). For the abundance of the isotopomer peaks, we summed the counts over twenty bins (from baseline to baseline). The ratio R and an $R_{standard}$ value of 0.011237 was used in Eq. (2) to determine $\delta^{13}C = -26.4 \pm 16.4‰$. A one sigma error bar of 16.4‰ is determined from the total number of ions collected and binomial statistics [1]. Our measurement closely resembles the $\delta^{13}C$ value of $-26.3 \pm 0.1‰$ measured independently on a high-precision IRMS [2]. For toluene, an identical data analysis procedure was used. No correction procedure for toluene fragmentation was performed because the laser power needed to produce such a low ion flux generates an insignificant number of fragment ions. A value of $-22.5 \pm 15.7‰$ was calculated from our experiments and again resembles the value obtained independently of $-27.5 \pm 0.1‰$ (see footnote 2).

4.2. Analog detection

To obtain high sensitivity, we typically ionize and detect many molecules simultaneously and utilize the signal averager in order to improve the signal-to-noise ratio of our mass spectra. It is important for us to extract the carbon isotope ratio from data obtained this way. We originally suspected that it would be necessary to include a correction factor for pulse pileup, but further analysis of the data demonstrated that we operate in a regime were the ion current reaching the detector is sufficiently small so that the gain is independent, within error, of the signal size.

Table 2
Carbon isotope ratios for toluene, toluene-d_8, and m-xylene-d_{10}

Molecule	Detection method	Laser shots	$\delta^{13}C$ (‰)
toluene	averaging [a]	100000	-38.3 ± 51.6
	ion counting	400000	-22.5 ± 15.7
	IRMS [c]	NA [b]	-27.5 ± 0.1
toluene-d_8	averaging	100000	-26.2 ± 31.6
	ion counting	313000	-26.4 ± 16.4
	IRMS [c]	NA [b]	-26.3 ± 0.1
m-xylene-d_{10}	averaging	100000	-15.0 ± 32.9
	IRMS [c]	NA [b]	-26.4 ± 0.1

[a] Corrected for fragmentation (see text).
[b] Not applicable.
[c] Determined independently using high-precision isotope ratio mass spectrometry [16].

A mixture of toluene, toluene-d_8, and m-xylene-d_{10} was leaked into the chamber through a needle valve. Laser power was adjusted to obtain strong parent ion and primary fragment ion signals. A typical 1000-shot averaged spectrum is shown in Fig. 3b. In addition to the isotopomer peaks for the three compounds, there are fragment peaks generated by either hydrogen or deuterium loss depending on the compound of origin. A series of 100 averaged spectra was recorded and transferred to a computer. The toluene-d_8 peaks were used as our calibrant for the analog signal measurements of the other two compounds. The isotope ratio R was calculated using Eq. (8). Peak centers for toluene-d_8, M^+ and $(M+1)^+$ peaks, were determined, and limits of integration were chosen such that the carbon isotope ratio corresponds to the value determined independently with an IRMS. The integration width was found to be smaller (70%) than the peak-to-peak distance. The isotope ratio R and $R_{standard} = 0.011237$ was used in Eq. (2) to determine the $\delta^{13}C$. Identical data analysis, using the previously determined integration widths, was performed for the m-xylene-d_{10} peaks. The results are given in Table 2, and it is clear that within error, the measurement of the carbon isotope ratio of m-xylene-d_{10} can be determined. Data sets with different ion currents reaching the detector were analyzed in a similar fashion, and produced consistent results. We were unable to find, however, a gain correction procedure that would consistently fit all of the data sets. The carbon isotope ratios for the

[1] Binomial statistics are used to define the counting distribution. For toluene-d_8, the probability of detecting an ion at 101 amu is 0.07266 and at 100 amu is 0.92484. These numbers were renormalized and the other isotopomer peaks were not considered. Therefore, the probability of detecting an ion at 101 amu is 0.07284 and at 100 amu is 0.92716. After many sets of n trials, the mean number of successes is $\nu = na$ and the standard deviation is $\sigma_\nu = (nab)^{1/2}$. From our data, 3275 ions were counted for 101 amu and 42775 ions were counted for 100 amu. This yields a standard deviation of 55 counts. Propogating this error results in a stadard deviation of 16.4‰.

[2] Analysis performed in duplicate on a dual-collector instrument at Global Geochemistry Corporation, Canoga Park.

various compounds can be varied by changing the limits of integration. This variation arises because noise added to the smaller $(M + 1)^+$ peak has a large effect on the isotope ratio when using the delta scale. By choosing the proper limits, we are reducing the effect of noise in the baseline. Because this noise is additive to the M^+ and $(M + 1)^+$ peaks alike and gain saturation is a function of ion current, gain saturation correction procedures could not be used to correct this error.

The error bars of the analog measurements are consistent with simulations performed on a computer. A simulated mass spectrum of toluene-d_8 with $\delta^{13}C = -26‰$ and mass resolution of 500 was generated and digitized to have roughly 65 data points defining the curve. This simulation closely approximates a typical mass spectrum for our instrument. White noise was added to these points and 2000 spectra were generated. The spectra were analyzed as above, and carbon isotope ratios determined. The addition of 1% white noise produced error bars of $\pm 31.2‰$, and the addition of 1.5% white noise produced error bars of $\pm 45.6‰$. This effect of adding white noise demonstrates the inherent limits to deriving carbon isotope ratios from digitized signals with small amounts of noise.

As signals become smaller, so too does the signal-to-noise ratio. To demonstrate that error bars on isotope ratio measurements increase with decreasing signal, we measured the carbon isotope ratio for gas-phase toluene-d_8 over a wide range of signal strengths. Because isotope ratios are determined by taking the ratio of two peak areas, statistical deviation of large signals is smaller than those for small signals. The data, as well as the $\pm 3\sigma$ envelope, for the range of signal strengths that we can observe are displayed in Fig. 4. To determine the $\pm 3\sigma$ envelope, the data was divided into 40 intervals of 0.1 spacing on the M^+ axis. The data from the $\pm 3\sigma$ error bar values for the 40 intervals were fit to $y = \pm c/x^{1/2}$. Although the envelope in Fig. 4 provides a guide to the eye, there is no physical justification for the form of this equation. Each data point is calculated from a 100-shot averaged spectrum retrieved from the oscilloscope.

4.3. Analog detection–fragmentation correction

For experiments performed with analog detection, the data for toluene are more complicated to interpret owing to the overlap between fragment peaks and parent peaks. Following the nomenclature used in

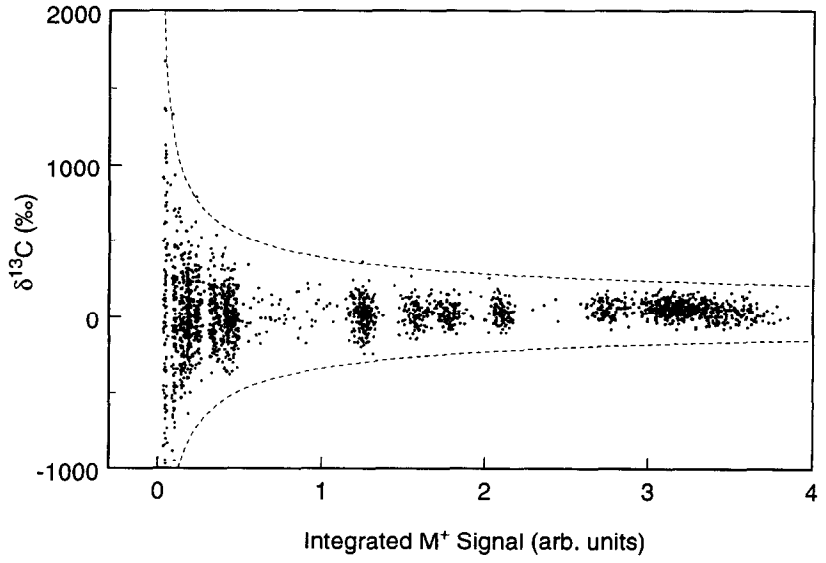

Fig. 4. Carbon isotope ratios for toluene-d_8 versus ion intensity measured at the detector assembly. Each data point is calculated for a 100-shot averaged spectrum with limits of integration equal to the peak-to-peak distance. The $\pm 3\sigma$ envelope is superimposed on the plot.

Fig. 2, the neutral, or ideal ion, distribution contains M and (M + 1). In the ion distributions, peak F^+ consists of fragments of M while peak M^+ includes fragments from (M + 1) and excludes loses to F^+. This redistribution of ions can be written as a system of equations, using X as a fragmentation factor,

$$F^+ = MX, \tag{10}$$

$$M^+ = M(1-X) + (M+1)X, \tag{11}$$

$$(M+1)^+ = (M+1)(1-X). \tag{12}$$

These three equations rearrange to solve for the fragmentation coefficient X and the ratio R,

$$X = \frac{(2F^+ + M^+) - \sqrt{(-2F^+ - M^+)^2 - 4F^+[F^+ + M^+ + (M+1)^+]}}{2[F^+ + M^+ + (M+1)^+]}, \tag{13}$$

$$R = \frac{(M+1)^+(X)}{F^+(1-X)}. \tag{14}$$

All spectra consisted of 1000-shot averages, and the limits of integration were determined from the toluene-d_8 calibration. A plot of the integrated M^+ values versus the integrated $(M+1)^+$ values shows that there is an offset in the data. This plot should extrapolate to the point (0, 0), but there appear to be extra $(M+1)^+$ ions. Previously, aniline (93 amu) was investigated in our instrument and residual contamination is a likely reason for this offset. The offset in the data was removed. The values from the M^+ and $(M+1)^+$ peaks of toluene-d_8 and *m*-xylene-d_{10} did extrapolate through the point (0, 0). The fragmentation coefficient X was found using Eq. (13) and the isotope ratio R determined using Eq. (14). The isotope ratio R and $R_{standard} = 0.011237$ was used in Eq. (2) to determine the $\delta^{13}C$ which is reported alongside the value measured independently with a high-precision isotope ratio mass spectrometer [16] in Table 2. The values for toluene are all consistent within error.

5. Concluding remarks

We have found that it is possible to determine accurate values of $\delta^{13}C$ for the aromatic compounds *m*-xylene-d_{10}, toluene-d_8, and toluene using REMPI followed by TOF mass spectrometry. The procedure for determining the $\delta^{13}C$ value using ion counting is simple, and the accuracy of the technique was confirmed by comparing the result with that obtained from a high-precision IRMS. The procedure used to determine the $\delta^{13}C$ value using analog detection of individual molecular species requires calibration with a standard to characterize the response of the detector and associated electronics. To determine the $\delta^{13}C$ value of a compound that has fragment ion peaks that overlap parent ion peaks, a deconvolution technique was successfully used. We achieve precisions, Table 2 and Fig. 5, of roughly ±15‰ for ion counting, ±35‰ for analog detection, and ±50‰ for analog detection with fragmentation correction. Because chemical fractionation of carbon isotopes in terrestrial environments is small and lies within these error bars [1–4], this technique is not suitable for studying terrestrial samples. However, carbon produced by the nucleosynthetic reactions of other stellar bodies is very different than our solar system mix of isotopes. In general, these differences are orders of magnitude greater than those produced by chemical fractionation and can be measured with our instrument. Interstellar graphite grains have been established to contain isotopically very anomalous carbon using an ion probe [10] and measurements are in progress to establish whether the sampled aromatics have an isotopic abundance that correlates with that of the bulk grain [17,18].

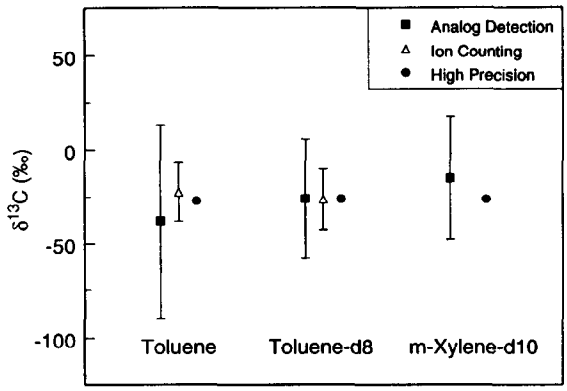

Fig. 5. Comparison of carbon isotope ratios measured by our time-of-flight method (analog detection and ion counting) and a commercial high-precision isotope ratio mass spectrometer.

Acknowledgements

We thank Neil Shafer-Ray and Rob Guettler for helpful discussions. CRM gratefully acknowledges

the Henkel Corporation for a predoctoral fellowship. This research was supported by the National Aeronautics and Space Administration (grant NAGW-3629).

References

[1] J. Hoefs, Stable isotope geochemistry, 3rd Ed. (Springer, Berlin, 1987).
[2] K. Lajtha and R.H. Michener, eds., Stable isotopes in ecology and environmental science (Blackwell, Oxford, 1994).
[3] M. Becchi, R. Aguilera, Y. Farizon, M.-M. Flament, H. Cusabianca and P. James, Rapid Commun. Mass Spectry. 8 (1994) 304.
[4] H.P. Taylor, J.R. O'Neil and I.R. Kaplan, eds., Stable isotope geochemistry: a tribute to Samuel Epstein, Special Publication No. 3 (Geochemical Society, 1991).
[5] H. Craig, Geochim. Cosmochim. Acta 12 (1957) 133.
[6] J. Santrock, S.A. Studley and J.M. Hayes, Anal. Chem. 57 (1985) 1444.
[7] D.E. Murnick and B.J. Peer, Science 263 (1994) 945.
[8] K.H. Freeman, J.M. Hayes, J.-M. Trendel and P. Albrecht, Nature 343 (1990) 254.
[9] D.A. Merritt and J.M. Hayes, Anal. Chem. 66 (1994) 2336.
[10] E. Anders and E. Zinner, Meteoritics 28 (1993) 490.
[11] L.J. Kovalenko, C.R. Maechling, S.J. Clemett, C.M.O'D. Alexander and R.N. Zare, Anal. Chem. 64 (1992) 682.
[12] S.J. Clemett, C.R. Maechling, R.N. Zare, P.D. Swan and R.M. Walker, Science 262 (1993) 721.
[13] W.C. Wiley and I.H. McLaren, Rev. Sci. Instr. 26 (1955) 1150.
[14] E. Anders and M. Ebihara, Geochim. Cosmochim. Acta 46 (1982) 2363.
[15] F. W. McLafferty and F. Turecek, Interpretation of mass spectra, 4th Ed. (University Science Books, Mill Valley, 1993).
[16] L. Giudicotti, M. Bassan, R. Pasqualotto and A. Sardella, Rev. Sci. Instr. 65 (1994) 247.
[17] S.J. Clemett, C.R. Maechling, R.N. Zare, S. Messenger, C.M.O'D. Alexander, X. Gao, P.D. Swan and R.M. Walker, Meteoritics 29 (1994) 457.
[18] S. Messenger, C.M.O'D. Alexander, X. Gao, P.D. Swan, R.M. Walker, S.J. Clemett, C.R. Maechling and R.N. Zare, Meteoritics 29 (1994) 502.